Effect of high strain rate on micro-indentation test in pure aluminum

H. Yamada[1], N. Ogasawara[1], Y. Shimizu[2], H. Horikawa[3], and H. Kobayashi[3]

[1]*National Defense Academy, School of Systems Engineering, 1-10-20 Hashirimizu Yokosuka Kanagawa, Japan*
[2]*National Defense Academy, Graduate Student, School of Systems Engineering, 1-10-20 Hashirimizu Yokosuka Kanagawa, Japan*
[3]*Osaka University, Graduate School of Engineering Science, 1-3 Machikaneyama Toyonaka Osaka, Japan*

Abstract. The indentation properties of pure aluminum (99.9%, 3N aluminum) and high purity aluminum (99.999%, 5N aluminum) with respect to the strain rate dependence of strength are experimentally investigated in order to clarify the effect of strain rate on the micro-indentation test. A micro-indentation test using a Berkovich indenter was performed at loading rates of 0.7, 7, and 70 mN/s. In all of the specimens, the indenter was loaded to a maximum value of 1200 mN, and then was maintained for 30 s. In the 3N specimen, the dependence of the loading rate on the load was slight at loading rates of 0.7 and 7 mN/s, whereas the load at the loading rate of 70 mN/s was higher than the loads at loading rates of 0.7 and 7 mN/s. On the other hand, the load for the 5N specimen increased with the increasing loading rate. Thus, the effect of the loading rate on the load-displacement curve for the 3N and 5N specimens was similar to the strain rate dependence of strength for theses metals. In addition, the micro-indentation test was demonstrated to be strongly affected by high strain rate at a loading rate of 70 mN/s.

1 Introduction

Instrumented indentation tests are widely used to investigate the elastic and plastic properties (indentation properties) of mechanical materials [1–3]. During an indentation experiment, a rigid indenter penetrates normally into a homogeneous solid, where the indentation load and displacement are continuously recorded during loading and unloading.

In the micro-indentation test, the hardness has been reported to increase with decreasing indentation depth [4,5] based on the strain rate. Doerner and Nix [4] pointed out that the material strength was affected by the strain rate in the indentation test. When the indentation test is performed at a constant displacement rate, the strain rate can be defined as follows:

$$\dot{\varepsilon} = c\left(\frac{1}{h}\frac{dh}{dt}\right) \tag{1}$$

where c is the material constant and h is the indentation depth. Thus, equation (1) indicates that the strain rate becomes very high as the indentation depth decreases.

In a previous study, the authors [6] have investigated the effect of high strain rate (dynamic strain rate) on indentation properties by comparing the results of a micro-indentation test at a loading rate of 70 mN/s and the results obtained by the finite element method (FEM) analysis using the pure copper (rolled copper and annealed copper) having strain rate dependence of strength. Figure 1 shows the load-displacement curves of the micro-indentation test and the FEM analysis for rolled copper and annealed copper [6]. The load-displacement curves obtained through the static-FEM analysis were inconsistent with those obtained through the micro-indentation test for both rolled copper and annealed copper. As a result of the static-FEM analysis, the strain rate at the early stage of testing reached the dynamic strain rate, approximately 10 s^{-1}, underneath the

sharp indenter in the micro-indentation test. The Cowper-Symonds model, which includes the strain rate dependence of strength, was then used in the dynamic-FEM analysis (LS-DYNA). The load-displacement curves calculated by the Cowper-Symonds model showed good agreement with the experimental results for both rolled copper and annealed copper. Thus, the indentation properties were affected by the dynamic strain rate.

In the present study, the indentation properties of the pure aluminum with the strain rate dependence of strength (99.9 mass% and 99.999 mass% pure aluminum) were experimentally investigated in order to clarify in greater detail the effect of high strain rate on the micro-indentation test.

2 Experimental details

2.1 Materials

Two types of pure aluminum with 99.9 mass% (hereinafter, mass% is referred to simply as %) purity (3N aluminum) and 99.999 mass% purity (5N aluminum: high-purity aluminum) were prepared. Compression test pieces with a gage length of 6.0 mm (l_s) and a diameter of 8.0 mm were machined using a lathe.

In the indentation test, the surface roughness of material was affected by the indentation properties. Thus, in the specimens using the indentation test, one surface was polished using emery paper (#2000) and was buffed with alumina pastes (diameters of 1 μm and 0.3 μm) to reduce the effect of surface roughness on the indentation properties.

All of the specimens were annealed at 623 K for 2 h (O temper) to remove the work-hardened layer [7] before the compression and the indentation test.
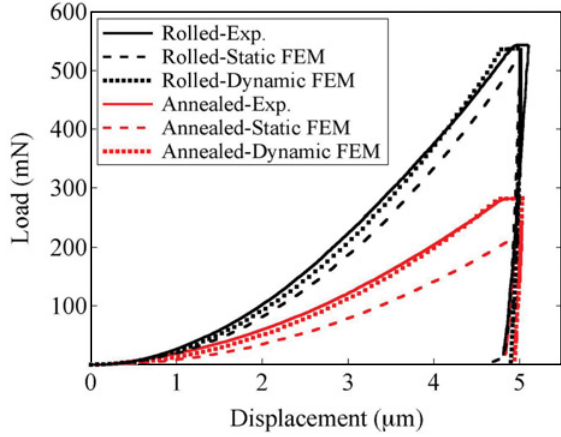
Fig. 1. Load-displacement curves obtained through a micro-indentation test and FEM analysis (static and dynamic) for rolled copper and annealed copper at a loading rate of 70 mN/s [6].
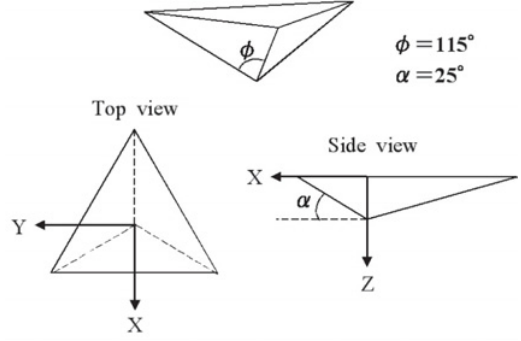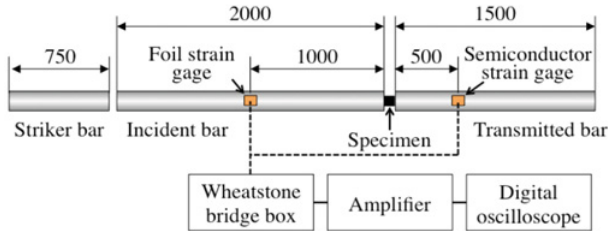

Fig. 2. Setup of the SHPB compression test. (Unit: mm)

2.2 Compression test

2.2.1 Quasi-static test

A quasi-static compression test (hereinafter referred to as the QS test) was carried out using an Instron-type universal testing machine at strain rates of 1.4×10^{-4}, 1.4×10^{-3}, and 1.4×10^{-2} s^{-1}.

2.2.2 Impact test

In the present study, the impact compression test was performed using the split Hopkinson pressure bar (SHPB) method [8,9]. Dynamic stress-strain curves can be obtained by incorporating the elementary one-dimensional elastic wave propagation theory [10–12] into the SHPB method.

Figure 2 shows the setup of the SHPB apparatus for the impact compression test. This apparatus consists primarily of a striker bar, an incident bar, a transmitted bar, and an associated recording system (Wheatstone bridge box, differential amplifier, and digital oscilloscope). These bars are 14 mm in diameter. The specimen is sandwiched between the incident bar and the transmitted bar.

When a striker bar impacts an incident bar, a compression stress wave propagates through the incident bar. When the compression stress wave reaches the specimen, part of the stress wave is reflected at the specimen, whereas the remaining part of the stress wave propagates through the transmitted bar. The stress waves can be measured by a foil strain gage (KYOWA, KFG-2-120-C1-11) and a semiconductor strain gage (KYOWA, KSP-1-350-E4) attached to the incident bar and the transmitted bar.

By applying the elementary one-dimensional elastic wave propagation theory, we can determine the nominal stress $\sigma(t)$, the nominal strain $\varepsilon(t)$, and the strain rate $\dot{\varepsilon}(t)$ in the specimen as follows:

$$\sigma(t) = \frac{AE}{A_s} \varepsilon_t(t) \tag{2}$$

$$\varepsilon(t) = \frac{2c_0}{l_s} \int_0^t [\varepsilon_i(t) - \varepsilon_t(t)] \, dt \tag{3}$$

$$\dot{\varepsilon}(t) = \frac{2c_0}{l_s} [\varepsilon_i(t) - \varepsilon_t(t)] \tag{4}$$

where A is the cross-sectional area of the specimen, A_s is the cross-sectional area of the elastic bars, E is Young's modulus of the incident and transmitted bars, C_0 is the velocity of the elastic wave in the incident and transmitted bars ($c_0 = \sqrt{E/\rho} \cong 5000$ m/s, ρ: density of the incident and transmitted bars), and $\varepsilon_i(t)$ and $\varepsilon_t(t)$ are the incident and transmitted waves, respectively.

In the present study, an average strain rate of the impact test was approximately 1.1×10^3 s^{-1}, as calculated by equation (4).

Both the QS test and the impact test were carried out at room temperature.

2.3 Micro-indentation test

Experiments were carried out using a micro-indentation testing machine, DUH201, supplied by SHIMADZU CORPORATION. The indenter was a Berkovich indenter with an edge angle of $\phi = 115°$, as shown Figure 3.

In the present study, the loading and unloading rates were 0.7, 7, and 70 mN/s at room temperature. The maximum load was 1200 mN, and then was maintained for 30 s before unloading (referred to hereinafter as the holding time).

All of the indentation tests were carried out in a stabilized case at a temperature variation of ±0.1 K. The number of tests was 10.
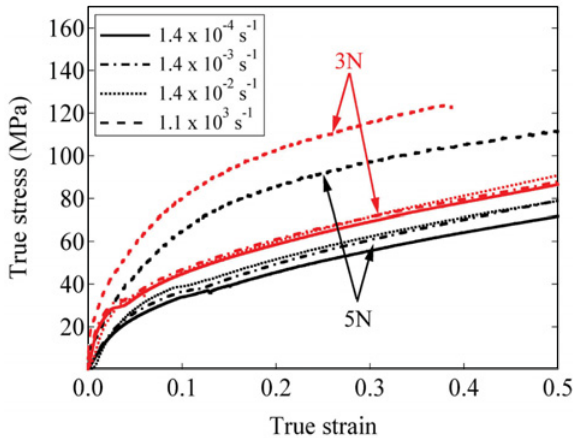

Fig. 3. Configuration of the Berkovich indenter.
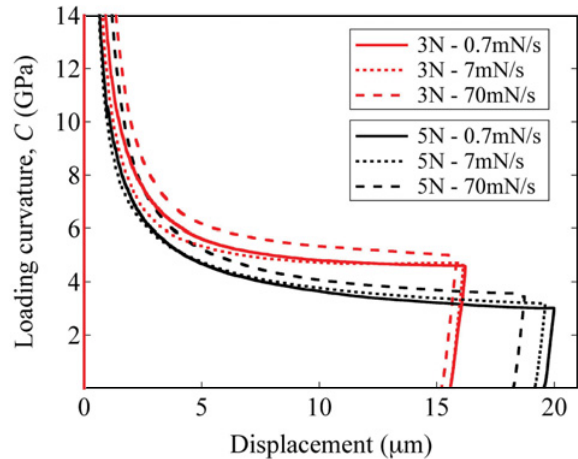
Fig. 4. True stress-strain curves for 3N and 5N aluminum in the QS test and the impact test.

Fig. 5. Load-displacement curves for 3N and 5N aluminum in the indentation test.

3 Results and discussion

3.1 Quasi-static and impact compression properties

Figure 4 shows the typical true stress-strain curves for 3N and 5N aluminum in the QS test and the impact test. As a result of the compression test, the flow stress decreased when the aluminum purity was increased from 99.9% to 99.999%, regardless of the strain rate.

In both 3N and 5N aluminum specimens, the flow stress was increased in the impact test as compared with the QS test. This trend is similar to the result reported by Holt *et al.* [13] whereby pure aluminum shows the strain rate sensitivity in the dynamic strain rate. However, in the QS test, the flow stress for 3N aluminum showed no change with increasing strain rate, whereas that for 5N aluminum increased, as described in detail later herein.

3.2 Indentation properties

3.2.1 Load-displacement relationship

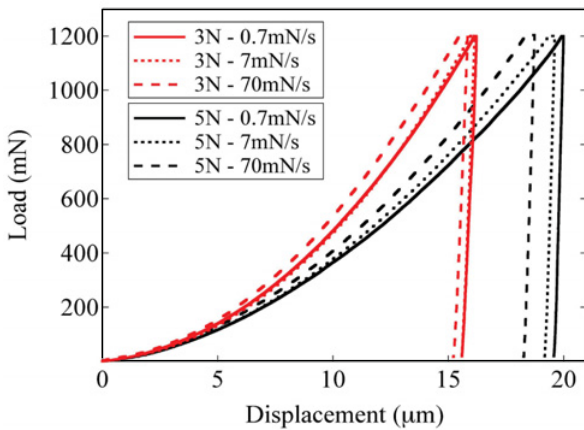Figure 5 shows the typical load-displacement curves for 3N and 5N aluminums in the indentation test. The load

Fig. 6. Loading curvature-displacement relationship for 3N and 5N aluminum in the indentation test.

of the indentation test was decreased when the aluminum purity was increased, as with the QS and the impact compression test results. During the loading process for 3N aluminum, the loads for the loading rates of 0.7 mN/s and 7mN/s were almost identical. However, the load for the loading rate of 70 mN/s was higher than those for the loading rates of 0.7 mN/s and 7mN/s. On the other hand, for the 5N aluminum, the load increased with increasing loading rate. Thus, it was revealed that the load of the micro-indentation test was affected by the loading rate.

3.2.2 Loading curvature-displacement relationship

In the indentation test, the loading segment of the load-displacement relationship obeys Kick's law as follows:

$$P = Ch^2 \qquad (5)$$

where C is the loading curvature, which is a constant value that depends on both the elasto-plastic properties of materials and the indenter angle.

Figure 6 shows the loading curvature-displacement relationship for 3N and 5N aluminum in the indentation test. For all of the loading rates, the loading curvature was not constant. The loading curvature was affected by the loading rate. The loading curvature decreased with increasing displacement immediately after indentation, and then this value was convergent, regardless of the loading rate. In both the 3N and 5N aluminum, the loading curvature value for the loading rate of 70 mN/s is larger than that for the loading rate of 0.7 mN/s and 7 mN/s.

3.2.3 Displacement during holding time at maximum load

Figure 7 shows the relationship between the displacement during the holding time at maximum load (referred to hereinafter as the holding displacement) and the loading rate for 3N and 5N aluminum in the indentation test. The holding displacement increased with increasing loading rate for both 3N and 5N aluminum. Based on this finding, stress-relaxation became increasingly difficult as the
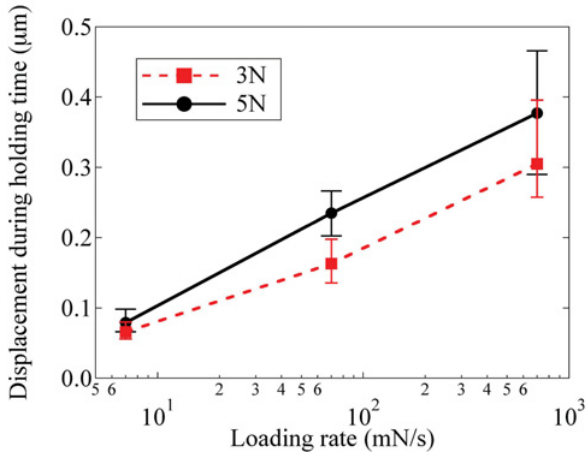
Fig. 7. Relationship between displacement during holding time at maximum load and loading rate for 3N and 5N aluminum in the indentation test.

loading rate increased. Thus, the holding displacement was increased, because this accumulation occurred in the holding time.

In addition, the holding displacement for the loading rate of 0.7 mN/s was approximately the same for 3N and 5N aluminum. However, the holding displacement for 5N aluminum was higher than that for 3N aluminum when the loading rate was higher than 7 mN/s. In recent studies [14, 15], the holding displacement was used by indentation creep test, which was affected by the testing temperature and the strain rate. In the present study, the effect of high strain rate on the holding displacement appeared for both 3N and 5N aluminum.

3.3 Relationship between loading rate and strain rate

In both 3N and 5N aluminum, the true stress-true strain relationship, as shown Figure 4, was investigated in detail, because the indentation properties were affected by the variation of the loading rate. Figure 8 shows the effect of strain rate on true stress at each true strain ($\varepsilon = 0.05, 0.15, 0.20$, and 0.30) in 3N and 5N aluminum. The strain rate dependence of the flow stress of 3N and 5N aluminum represents using the logarithm of the strain rate, as shown Figure 8. Comparing the true stress at each true strain for 3N aluminum and 5N aluminum revealed that the trend of the QS test was different.

Thus, the rate of increase in the true stress at each true strain, which was caused by the increasing strain rate, was calculated using the least squares method. In the present study, this rate of increase was defined as the strain rate sensitivity. Table 1 shows the strain rate sensitivity at each true strain obtained from Figure 8 for 3N and 5N aluminum, where α and β are the strain rate sensitivity of the QS test and the strain rate sensitivity of the comparison with QS (1.4×10^{-2} s^{-1}) and the impact test, respectively. In both 3N and 5N aluminum, β, which indicates that the strain rate dependence of strength between the QS and impact deformation, was high, as shown Section 3.1.

On the other hand, for the 3N aluminum, α was very small and did not exhibit the strain rate dependence of
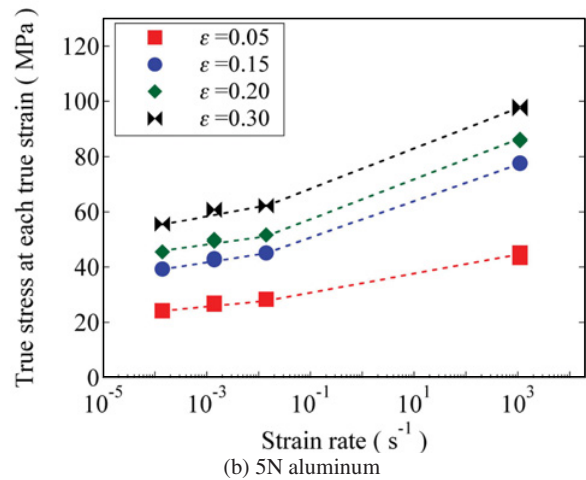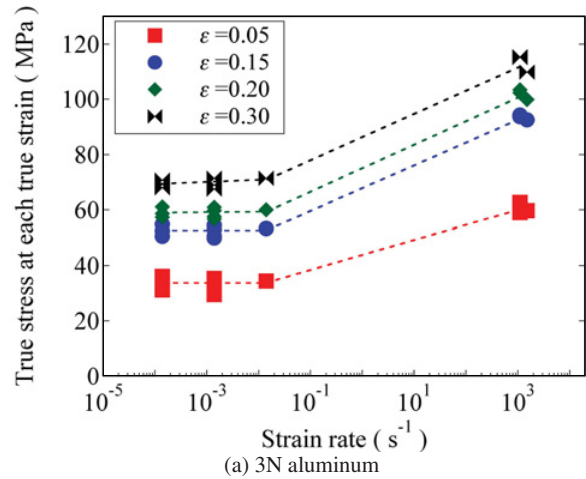

(a) 3N aluminum

(b) 5N aluminum

Fig. 8. Effect of strain rate on true stress at each true strain in 3N and 5N aluminum.

Table 1. Strain rate sensitivity at each true strain obtained from Fig. 8 in 3N and 5N aluminum. α: QS test, β: comparison with QS (1.4×10^{-2} s^{-1}) and the impact test.

	3N		5N	
ε	α	β	α	β
0.05	0.00	2.29	0.91	1.41
0.15	0.03	3.53	1.25	2.89
0.20	0.12	3.67	1.34	3.05
0.30	0.38	3.68	1.45	3.15

strength in the QS test. Compared to 3N aluminum, the value of α for the 5N aluminum was higher. It has been reported [13] that the effect of decreased alloying or purity is a decrease in the athermal stress component, which induce increased strain rate sensitivity in O tempered aluminum using the thermally activated process concept. Thus, the results obtained in the present study were related to aluminum purity.

In the experiments, the effect of loading rate on load during indentation, as shown Figure 5, was in agreement with the trend of the strain rate dependence of flow stress for the QS test for loading rates of 0.7 mN/s and 7 mN/s for 3N and 5N aluminum. A loading rate of up to 7 mN/s may reveal the QS strain rate. On the other hand, the indentation

test for a loading rate of 70 mN/s reached a high strain rate, indicating a dynamic strain rate, in pure aluminum, as shown in the previous study using pure copper [6]. Thus, the micro-indentation test was strongly affected by dynamic strain rate at a loading rate of 70 mN/s.

4 Summary

In order to clarify the effect of high strain rate on the micro-indentation test, the indentation properties of pure aluminum with strain rate dependence of strength was investigated experimentally. The obtained results are summarized as follows. (1) The strain rate dependence of flow stress for 5N aluminum was higher than that for 3N aluminum in both the QS test and the impact test. (2) In 3N and 5N aluminum, the effect of loading rate on the indentation properties was similar to the strain rate dependence of flow stress. (3) The micro-indentation test was strongly affected by the dynamic strain rate at a loading rate of 70 mN/s.

Acknowledgements

References

1. Y.T. Cheng, C.M. Cheng, Mater. Sci. Eng. **R44**, 91 (2004).
2. A. Gouldstone, N. Chollacoop, M. Dao, J. Li, A.M. Minor, Y.-L. Shen, Acta Mater. **55**, 4015 (2007).
3. N. Ogasawara, X. Chen, N. Chiba, J. Mater. Res., **21**, 947 (2006).
4. M.F. Doerner, W.D. Nix, J. Mater. Res., **1**, 601 (1986).
5. E. Harsono, S. Swaddiwudhipong, Z.S. Li, L. Shen, Int. J. Solids Structures, **48**, 972 (2011).
6. H. Yamada, N. Ogasawara, Y. Shimizu, *Proc. JSME 24th Comp. Mech. Div. Conf.*, 578 (2011).
7. N. Ogasawara, C. Kuramochi, W. Makiguchi, N. Chiba, Trans. JSME A, **69**, 805 (2003).
8. H. Kolsky, *Proc. Phys. Soc. B*, **62**, 676 (1949).
9. B. Hopkinson, Phil. Trans. A, **213**, 437(1914).
10. K. Ogawa, J. J. Inst. of L. M., **51**, 175 (2001) 175.
11. K. Ogawa, H. Kobayashi, F. Sugiyama, K. Horikawa, JSME Int. J. A, **48**, 228 (2005).
12. W. Johnson: *IMPACT STRENGTH OF MATERIALS*, (Edward Arnold, London, 1972).
13. D.L. Holt, S.G. Babcock, S.J. Green, C.J. Maiden, Trans. of ASM, **60**, 152 (1967).
14. R. Goodall, T.W. Clyne, Acta Mater., **54**, 5489 (2006).
15. K. Sakaue, S. Okazaki, T. Ogawa, Trans. JSME A, **75**, 1045 (2009).